Investigation of multispectral SF_6 stimulated Raman scattering laser

Chencheng Shen (沈陈诚)[1,2], Xianglong Cai (蔡向龙)[1,3], Youbao Sang (桑友宝)[1,2], Tiancheng Zheng (郑天成)[1,2], Zhonghui Li (李仲慧)[1], Dong Liu (刘 栋)[1], Wanfa Liu (刘万发)[1], and Jingwei Guo (郭敬为)[1,*]

[1]*Key Laboratory of Chemical Lasers, Dalian Institute of Chemical Physics, Chinese Academy of Sciences, Dalian 116023, China*
[2]*University of Chinese Academy of Sciences, Beijing 100049, China*
[3]*School of Science, Changchun University of Science and Technology, Changchun 130022, China*
**Corresponding author: jingweiguo@dicp.ac.cn*

Received November 4, 2019; accepted January 3, 2020; posted online April 21, 2020

In this work, SF_6 as a Raman-active medium is investigated to generate a multispectral Raman laser by the combination of cascade stimulated Raman scattering (SRS) and four wave mixing. The Raman frequency comb from the 10th-order anti-Stokes to the 9th-order Stokes was generated, and its spectral range covered 377–846 nm. The photon conversion efficiency of 16.4% for the first Stokes was achieved, and the Raman gain coefficient at 1.5 MPa of SF_6 under the 532 nm pump laser was calculated to be 0.83 cm/GW by the SRS threshold comparison with H_2. Using helium as the carrier gas, the thermal effect of the SF_6 Raman laser was improved dramatically under a repetition rate of 10 Hz.

Keywords: multispectral Raman laser; Raman frequency comb; stimulated Raman scattering; four wave mixing; conversion efficiency.
doi: 10.3788/COL202018.051402.

An optical frequency comb (OFC) normally covers very broad spectral range and is composed of a series of phase-locked spectral lines with equal spacing in the frequency domain. OFC has very broad applications in attosecond pulse generations[1,2], ultrafast process investigations[3], terahertz imaging[4], precision distance measurements[5], etc. There are several ways to generate OFC, such as micro resonator in combination with laser media with wide fluorescence spectral range[6], cascade four wave mixing (FWM), and cascade stimulated Raman scattering (SRS)[7–9]. However, for OFC generated by SRS, in order to achieve the phase stable spectral lines, a single longitudinal mode pump laser is required; in addition, phase-locked S1 seed light will benefit the phase stability of OFC. In this work, the combination of cascade SRS and cascade FWM of SF_6 pumped by an unseeded Nd-doped yttrium aluminum garnet (Nd:YAG) laser was used to generate the multispectral Raman laser (Raman frequency comb). Although this Raman frequency comb is not OFC, due to the phase instability, it still could provide useful guidance for the OFC generated by the single longitudinal mode laser pumped SF_6. Furthermore, the multispectral characteristic of the Raman frequency comb makes it a great application for laser radar, laser displaying, spectral calibrations, optical-electron counter measurements, Raman spectrometers, etc.[10–13].

SRS is an efficient method to broaden the spectral range of a high peak power laser. Both solid and gaseous media could be used for Raman conversion. Solid-state Raman media have the advantages of high gain coefficient, low threshold, compact volume, etc., and their Raman shifts are almost all around 1000 cm^{-1}. On the contrary, gaseous Raman media have relatively lower Raman gain coefficients, higher threshold, etc. Their Raman shifts cover a large range, such as 4155 cm^{-1} for the vibrational Raman mode of H_2, 2917 cm^{-1} for CH_4, and 1388 cm^{-1} for CO_2, so the spectra of gaseous Raman lasers are more abundant and cover a wider range. Furthermore, the damage threshold of gaseous Raman media is much higher than that of solid media. In spite of a relatively low gain coefficient, by the applications of intra-cavity or multiple-pass configuration, the thresholds of gaseous SRS could also be reduced significantly[14–16]. Also, the conversion efficiency of gaseous SRS could be higher than 80%[17]. SRS can also be efficiently enhanced by the pre-excitation of coherent vibration or electronic resonance. A recent work showed that when the probe laser was resonant with the electronic transitions, vibration Raman scattering could be enhanced by at least two orders of magnitude[18]. As the first Stokes (S1) Raman conversion efficiency increases, the higher orders of Stokes and anti-Stokes Raman tend to be generated[19]. By a series of cascade SRS, a low frequency Raman frequency comb could be generated; while by a series of cascade FWM, a high frequency Raman frequency comb could be generated. The scheme of cascade SRS and FWM is illustrated in Fig. 1.

H_2 and D_2 have been successfully used to generate a Raman frequency comb due to relatively large gain coefficients and small Raman shifts of their rotational modes[9,20]. To generate a Raman frequency comb with a dense spectral line, media with a small Raman shift are required. For SF_6 as a Raman-active medium, transient SRS was studied by Wittmann's group. Its vibrational mode A_{1g} has a relatively small Raman shift of 775 cm^{-1},

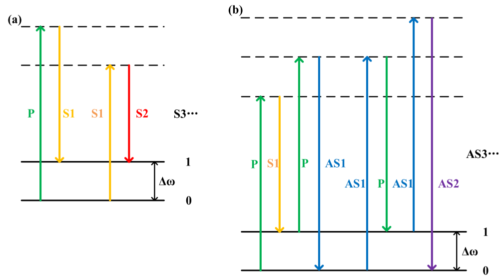

Fig. 1. Schematic diagram of (a) cascade SRS and (b) cascade FWM.

and the Raman conversion efficiency they obtained was nearly 100% in the impulsively excited SF_6 gas[21–23]. Although the rotational mode of H_2 also has a smaller Raman shift (587 cm^{-1}), it is not convenient to generate a Raman frequency comb with an abundant spectral line due to the competition of its vibrational mode. SF_6 is one of the best electron absorption media, even friction of SF_6 is ionized by the strong laser; it will not form plasma by the avalanche effect[24]. Therefore, SF_6 could work under extremely high pumping intensity, while other molecules such as H_2, D_2, and CH_4 suffer serious laser induced breakdown under extremely high pumping intensity, and consequently, Raman conversion efficiencies decrease dramatically. In this work, SF_6 was used as a medium to study the multispectral Raman laser, and for the first time, to the best of our knowledge, steady-state SRS of SF_6 was investigated by using light of 532 nm as the pump source. The multispectral Raman laser covering the visible light range and the Raman frequency comb with up to 20 frequencies was generated. The pressure of SF_6 was optimized to achieve better Raman conversion efficiency, and photon conversion efficiencies of 16.4% for S1, 8.4% for the second Stokes (S2), 4.9% for the third Stokes (S3), and 2.0% for the first anti-Stokes (AS1) were obtained. The S1 Raman gain coefficient at 1.5 MPa of SF_6 under the 532 nm pump laser was calculated to be 0.83 cm/GW.

In this work, the second harmonic at 532 nm generated by a *Q*-switched Nd:YAG solid-state laser (Beamtech Optronics Co., Ltd. SGR-20) was used as the pump source. The laser beam divergence angle was about 1 mrad, and the laser beam diameter was about 10 mm. The line width was 1 cm^{-1}, and the pulse width was 10 ns. The maximum repetition rate of this laser was 20 Hz, and it could operate at repetition rates of 10 Hz, 5 Hz, and 1 Hz as well. The output beam passed through an optical isolator consisting of a polarizing beam splitter prism (PBSP) and a quarter-wave plate. It was used to isolate the backward SRS light and the stimulated Brillouin scattering (SBS) light generated in the experiment; also, the pump power of SRS light could be adjusted continuously by rotating the half-wave plate in front of the optical isolator. Then, the laser beam passed through plano-convex lens L1 and was focused approximately at the center of the Raman cell. The focal length of L1 was 1.5 m. The Raman cell, made of 1.8 m stainless steel tube and JGS1 fused silica windows, was filled with SF_6 gas of 99.995% purity. The pressure of SF_6 in the Raman cell was adjusted from 0.7 to 1.5 MPa. The experimental setup is illustrated in Fig. 2.

The SRS and FWM processes occurred in the Raman cell, outputting the remaining pump laser and other Raman components through the exit window. The output beam was collimated by another plano-convex lens L2 of 1.5 m focal length. Then, the SRS components of different wavelengths were separated by a Pellin–Broca prism and recorded with a camera (see Fig. 2). Then, a spectrometer (Horiba JY iHR-320) was used to record the spectra of the Stokes and anti-Stokes laser lines, and an energy meter (Gentec-EO QE50LP-H-MB-D0) was used to measure their energies at each wavelength separately.

As shown in Fig. 3(a), by using the 532 nm laser as a pump source, the multispectral Raman laser covering the visible light range from 377.2 nm to 847.3 nm was generated with 1.5 MPa SF_6 gas under pumping energy of about 100 mJ. In our work, from the 10th-order anti-Stokes up to the 9th-order Stokes, Raman frequency comb components were observed.

The Raman shift of SF_6 is 775 cm^{-1}, and, according to this, the wavelengths of each spectral line of the generated Raman frequency comb under the 532 nm laser pump are calculated and listed in Table 1, which are consistent with

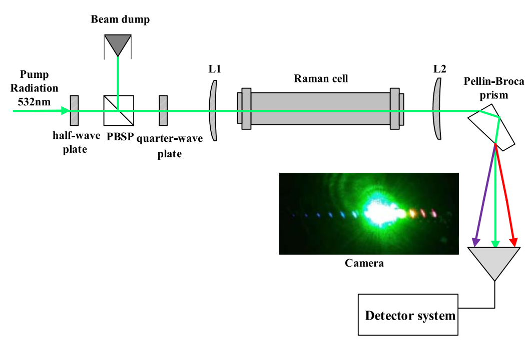

Fig. 2. Schematic diagram of the experimental setup.

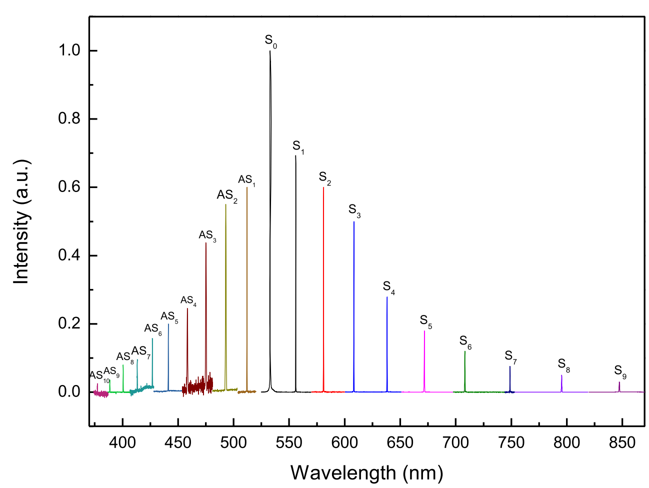

Fig. 3. Spectra of the generated Raman frequency comb under the 532 nm pump for SF_6 gas.

Table 1. SF_6 SRS Line's Wavelength of 532 nm Laser Pump

Stokes Order	Wavelength Calculated (nm)	Wavelength Measured (nm)	Stokes Order	Wavelength Calculated (nm)	Wavelength Measured (nm)
S0	532.1	532.9	AS1	511.0	512.0
S1	555.0	556.0	AS2	491.6	493.0
S2	579.9	581.0	AS3	473.5	475.1
S3	607.2	608.2	AS4	456.8	458.3
S4	637.2	638.2	AS5	441.1	441.2
S5	670.3	671.8	AS6	426.6	426.9
S6	707.0	708.2	AS7	412.9	413.3
S7	748.0	748.8	AS8	400.1	400.6
S8	794.1	795.4	AS9	388.1	388.6
S9	846.1	847.3	AS10	376.7	377.2

the spectrum recorded by the spectrometer. The slight differences between the measured Raman wavelengths and the calculated results came from the small errors from the spectrometer.

The Stokes and anti-Stokes pulse shapes are also investigated and shown in Fig. 4. The pulse-width narrowing effect was observed in the SRS process of SF_6. It was shown that the higher-order Stokes laser had the smaller linewidth.

The SF_6 SRS photon conversion efficiencies of the first Stokes (S1) under different pressures were investigated. The pressure of SF_6 in the Raman cell was raised from 0.7 MPa to 1.5 MPa, and the photon conversion efficiencies were measured and presented in Fig. 5, respectively. It can be clearly seen that all the photon conversion efficiencies under different pressures of SF_6 increased with the pulse energy of the pump laser up to 100 mJ. Although the photon conversion efficiency showed the tendency to increase, due to the limitation of our experimental condition, the maximum pulse energy of the pump laser was ~100 mJ. The thresholds of SRS decreased with the increase of the pressure in the Raman cell of SF_6, while

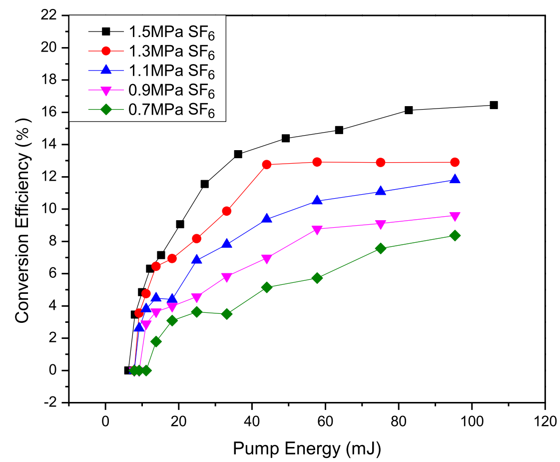

Fig. 5. S1 photon conversion efficiencies under different pump energies and pressures of SF_6.

the S1 photon conversion efficiencies significantly increased with pressure of SF_6. This result may be explained by the fact that the Raman gain coefficient increases with the pressure. The conversion efficiencies are likely going to increase further with the pressure of SF_6, but the higher pressure may cause the liquefaction of SF_6, so the maximum pressure of SF_6 in our study is 1.5 MPa.

As shown in Fig. 6, the photon conversion efficiencies of S1, S2, S3, and AS1 were investigated for 1.5 MPa SF_6, while other Raman components had intensities too weak to be measured by the energy meter. In this study, at high pump energy, the maximum photon conversion efficiencies of S1, S2, S3, and AS1 were 16.4%, 8.4%, 4.8%, and 2.0%, respectively.

With the same experimental setup, the Raman cell was filled with 1.5 MPa H_2 of 99.999% purity. In order to calculate the S1 Raman gain coefficient of SF_6, the S1 conversion efficiencies of H_2 were measured and presented in Fig. 7. For the convenience of comparison, the S1 conversion efficiency curve of SF_6 was also included in

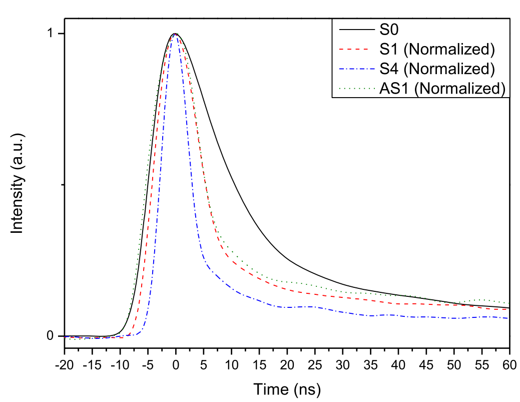

Fig. 4. Pulse shapes of the S0, AS1 (normalized), S1 (normalized), and S4 (normalized) laser beams.

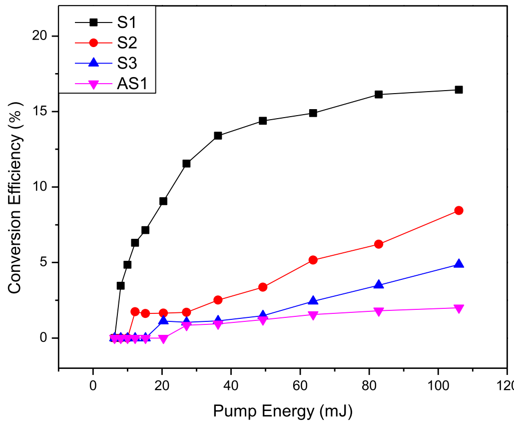

Fig. 6. Photon conversion efficiencies of S1, S2, S3, and AS1 versus the pump energies at 1.5 MPa SF_6.

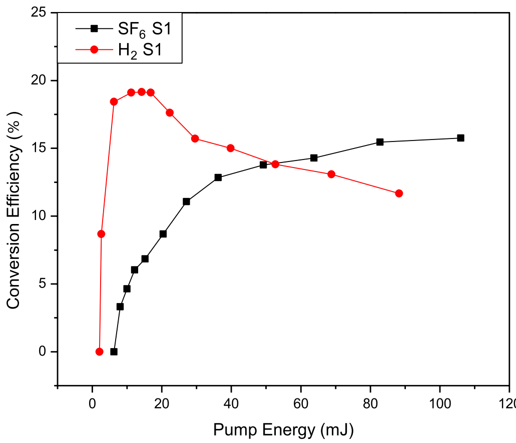

Fig. 7. S1 conversion efficiencies versus the pump energies under 1.5 MPa H_2 and SF_6.

Fig. 7. The small signal amplification of SRS could be expressed as[25]

$$I_S(L) = I_S(0)\exp(g_s I_P L), \tag{1}$$

where I_S is the intensity of S1, g_s is the Raman gain coefficient, I_P is the intensity of the pump laser, and L is the interaction length in stimulated Raman gain. This formula is applicable for the SRS conversion around the threshold. As shown in Fig. 7, H_2 had the threshold energy of about 2.1 mJ, and SF_6 had the threshold energy of about 6.8 mJ. Therefore, the S1 stimulated Raman gain coefficient of SF_6 is about 31% of that of H_2 at the pressure of 1.5 MPa.

The S1 Raman gain coefficient of 1.5 MPa H_2 can be calculated by the following formula[26]:

$$g_s = \frac{8\pi c^2 \Delta N}{n_s \hbar {\omega_s}^3 \Delta\nu_R}\left(\frac{\mathrm{d}\sigma}{\mathrm{d}\Omega}\right), \tag{2}$$

where ΔN is the population density difference between the initial and final states, n_s is the refractive index, $\Delta\nu_R$ is the linewidth (FWHM) of the Raman amplifier gain profile, ω_s is angular frequency of Stokes photons, and $\mathrm{d}\sigma/\mathrm{d}\Omega$ is the differential cross section for Raman scattering. For 1.5 MPa H_2, $\mathrm{d}\sigma/\mathrm{d}\Omega = 7.9\times10^{-35}\ \mathrm{m}^2/\mathrm{sr}$[27] under 532 nm laser pump, and $\Delta\nu_R$ can be estimated by the empirical equation as[28]

$$\Delta\nu_R = \frac{309}{\rho}\left(\frac{T}{298}\right)^{0.92} + \left[51.8 + 0.152(T-298) + 4.85\times10^{-4}(T-298)^2\right]\rho, \tag{3}$$

where ρ is the density, and T is the temperature.

According to our calculations, the forward S1 SRS gain coefficient of H_2 at the pressure of 1.5 MPa is 2.68 cm/GW. Thus, the stimulated Raman gain coefficient of SF_6 S1 is about 0.83 cm/GW.

In this work, it is found that when the repetition rate of the pump laser was increased to 10 Hz, the S1 conversion efficiency of SF_6 would reduce significantly with higher fluctuation (error bar), and the beam quality was also degraded. It confirms that a thermal defocusing effect was produced with the high pulse repetition rate of the pump laser for SF_6 gas.

Previous work has shown that the thermal effect could be reduced by adding helium (He) into the SRS process[29]. Therefore, different pressures of He were added as carrier gas in the Raman cell. Figure 8 shows the S1 conversion efficiencies for the mixed gas and pure SF_6 under the repetition rate of 10 Hz. The root mean square (RMS) values of 200 pulses were also recorded to characterize the stability of the SRS output energy. The results of this study indicate that with the increase of He carrier gas, the conversion efficiency and energy stability of S1 were both remarkably improved, so it confirms that adding He can contribute to reducing the thermal effect of SF_6 under the higher pump laser power and repetition rate. The thermal conductivity of SF_6 is 0.014 $\mathrm{W/(m\cdot K)}$, and the

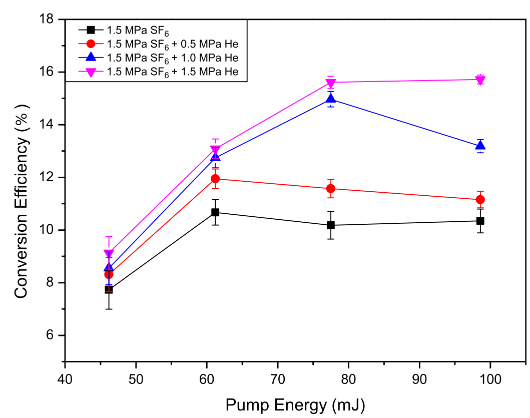

Fig. 8. S1 conversion efficiencies versus the pump energies of 1.5 MPa SF_6 with He carrier gas under a repetition rate of 10 Hz. The pressures of He were 0 MPa, 0.5 MPa, 1.0 MPa, and 1.5 MPa, respectively. The vertical lines represent the error bars.

thermal conductivity of He is 0.144 $W/(m \cdot K)$, which is ten times that of SF_6, so it is effective for improving the heat transfer capacity of the medium by filling the Raman cell with He carrier gas.

In conclusion, pumped by the pulsed 532 nm laser, SF_6 was used as a Raman medium, and the multispectral Raman laser covering almost the whole visible light range and the Raman frequency comb up to 9 order Stokes and 10 order anti-Stokes was successfully generated. The spectral range covered 377–846 nm. The spacing between the adjacent frequencies of the Raman frequency comb is 775 cm^{-1}, which corresponds to the Raman shift of the strongest Raman mode of SF_6. If a laser with a shorter wavelength (such as 355 nm) was used as the pump source, the Raman frequency comb with higher frequencies can be obtained; while if the laser with a longer wavelength (such as 1064 nm) was used as the pump source, the Raman frequency comb with lower frequencies can be obtained. By comparison with SRS of H_2, the S1 Raman gain coefficient of SF_6 was calculated to be 0.83 cm/GW. The combination properties of a decent Raman gain coefficient and a relatively smaller Raman shift enable the generation of a multispectral Raman laser with 20 frequencies. The Raman gain coefficient was found to significantly increase with the pressure of SF_6 up to 1.5 MPa, and the maximum S1 photon conversion efficiency was 16.4%, with conversion efficiencies of 8.4% and 4.8% achieved for S2 and S3, respectively. These are the highest conversion efficiencies for SRS of SF_6, to the best of our knowledge. Because the thermal conductivity of SF_6 is very low, therefore SF_6 could not stand the operation of a repetition rate of 10 Hz. If 1.5 MPa He was added to the Raman cell, the thermal effect was reduced dramatically, and the SF_6 Raman laser could operate at a repetition rate of 10 Hz without
decreasing the S1 Raman conversion efficiency.

This work was supported by the National Natural Science Foundation of China (NSFC) (Nos. 11475177 and 61505210) and the Key Laboratory Innovation Foundation (No. KLCL-2018-N11).

References

1. P. M. Paul, E. S. Toma, P. Breger, G. Mullot, F. Auge, P. Balcou, H. G. Muller, and P. Agostini, Science **292**, 1689 (2001).
2. S. Baker, A. Walmsley, J. W. G. Tisch, and J. P. Marangos, Nat. Photon. **5**, 664 (2011).
3. F. Krausz and M. Ivanov, Rev. Mod. Phys. **81**, 163 (2009).
4. D. Shao, C. Yao, T. Zhou, R. Zhang, Z. Fu, S. Zhuang, and J. Cao, Chin. Opt. Lett. **17**, 041101 (2019).
5. I. Coddington, W. C. Swann, L. Nenadovic, and N. R. Newbury, Nat. Photon. **3**, 351 (2009).
6. X. Xue and A. M. Weiner, Front. Optoelectron. **9**, 238 (2016).
7. T. J. Kippenberg, R. Holzwarth, and S. A. Diddams, Science **332**, 555 (2011).
8. A. Carrasco-Sanz, S. Martin-Lopez, M. Gonzalez-Herraez, P. Corredera, M. L. Hernanz, and L. Abrardi, Opt. Commun. **281**, 2948 (2008).
9. A. Abdolvand, A. M. Walser, M. Ziemienczuk, T. Nguyen, and P. S. J. Russell, Opt. Lett. **37**, 4362 (2012).
10. Y. W. Chen, E. Räikkönen, S. Kaasalainen, J. Suomalainen, T. Hakala, J. Hyyppa, and R. Z. Chen, Sensors **10**, 7057 (2010).
11. K. Martinez, J. Cupitt, D. Saunders, and R. Pillay, Proc. IEEE **90**, 28 (2002).
12. P. Carcagnì, A. D. Patria, R. Fontana, M. Greco, M. Mastroianni, M. Materazzi, E. Pampaloni, and L. Pezzati, Opt. Laser Eng. **45**, 360 (2007).
13. X. Li, Chin. Opt. Lett. **14**, 021404 (2016).
14. D. Zhou, J. Guo, C. Zhou, J. Liu, D. Liu, and Y. Jin, Opt. Commun. **356**, 49 (2015).
15. X. Cai, J. Guo, C. Zhou, D. Zhou, J. Liu, and L. Gui, Chin. Phys. Lett. **32**, 114207 (2015).
16. D. Liu, X. Cai, Z. Li, X. Xia, D. Zhou, G. Li, H. Cai, J. Guo, and Y. Jin, Opt. Commun. **379**, 36 (2016).
17. J. L. Carlsten, J. M. Telle, and R. G. Wenzel, Opt. Lett. **9**, 353 (1984).
18. B. Xu, J. P. Yao, Y. X. Wan, J. M. Chen, Z. X. Liu, F. B. Zhang, W. Chu, and Y. Cheng, Opt. Express **27**, 18262 (2019).
19. Z. Chu, U. N. Singh, and T. D. Wilkerson, Appl. Opt. **30**, 4350 (1991).
20. P. Hosseini, A. Abdolvand, and P. S. J. Russell, Opt. Lett. **41**, 5543 (2016).
21. A. Nazarkin, G. Korn, M. Wittmann, and T. Elsaesser, Phys. Rev. Lett. **83**, 2560 (1999).
22. M. Wittmann, A. Nazarkin, and G. Korn, Phys. Rev. Lett. **84**, 5508 (2000).
23. M. Wittmann, A. Nazarkin, and G. Korn, Opt. Lett. **26**, 298 (2001).
24. M. Yousfi, P. Segur, and T. Vassiliadis, J. Phys. D: Appl. Phys. **18**, 359 (1985).
25. D. Von der Linde, M. Maier, and W. Kaiser, Phys. Rev. **178**, 11 (1969).
26. W. Kaiser and M. Maier, *Stimulated Rayleigh, Brillouin and Raman Spectroscopy* (North Holland, 1972).
27. D. C. Hanna, D. J. Pointer, and D. J. Pratt, IEEE J. Quantum Electron. **22**, 332 (1986).
28. W. K. Bischel and M. J. Dyer, Phys. Rev. A **33**, 3113 (1986).
29. A. D. Papayannis, G. N. Tsikrikas, and A. A. Serafetinides, Appl. Phys. B **67**, 563 (1998).